Sustainable Chemical Engineering
http://ojs.wiserpub.com/index.php/SCE/

UNIVERSAL WISER PUBLISHER

Research Article

Valorization of Fired Clay Bricks Debris (grog) Using Egg Shell and Coconut Shell in the Synthesis of an Ecological Compressed Earth Blocks: Microstructure and Engineering Properties

Liyong Luc Arnold [1,2*], Tchuifon Tchuifon Donald Raoul [1], Fotsop Cyrille Ghislain [3], Linda Lekuna Duna [2], Tchedele Langollo Yannick [2], Nsouandele Jean Luc [1]

[1]Laboratory of Chemical Engineering and Industrial Bio-Processes, National Higher Polytechnic School of Douala, University of Douala, P.O. Box 2701, Douala, Cameroon
[2]Laboratory of Materials Analysis, Local Materials Promotion Authority, Yaounde, Cameroon
[3]Institute of Chemistry, Faculty of Process and Systems Engineering, Universität Platz 2, 39106 Magdeburg, Germany
Email: arnoldliyong89@gmail.com

Received: 20 June 2024; **Revised:** 2 August 2024; **Accepted:** 6 August 2024

Abstract: The aim of this work is to valorize fired clay brick debris (grog, CH) by using egg and coconut shells in the production of eco-friendly compressed earth bricks for sustainable building materials. Samples were cured at ambient temperature (23 ± 3 °C) and obtained by altering different percentages of (CO) and (CN) at 13%, 26% and 40%, respectively; while another mix design of calcined eggshell and coconut shell were incorporated together into the grog powder. Some comprehensive physico-mechanical properties such as water absorption (WA), bulk density (BD), apparent porosity (AP), moisture content (MC), compressive strength (σ) and elastic modulus (EM) were carried out. Chemical composition, X-ray diffraction (XRD) analysis, Fourier Transformed Infra-red (FT-IR), Energy Dispersive X-ray (EDX) analysis and Scanning Electron Microscopy (SEM) were studied. Results show an increase in compressive strength with increasing percentages of calcined eggshell, from 87CH 13CO, 74CH 26CO, 60CH 40CO as 1.38, 2.70, 3.88 MPa, respectively. For 87CH 13CN, 74CH 26CN, 60CH 40CN coconut shell addition show an increase in the percentages of compressive strength. The bulk density decreases with the increase in percentages of calcined eggshell and coconut shell and the percentage of grog decrease. Linear correlation equtions between mechanical properties and mix proportion were determined. SEM micrograph shows a dense microstructure with an agglomeration on the structure. Results obtained indicates an improvement in the engineering properties due to the addition of eggshell waste and these improved properties are suitable to enhance sustainable eco-friendly building materials.

Keywords: mechanical properties, grog, eggshell, coconut shell, linear correlation, microstructure

1. Introduction

Recently, the global construction industry has been faced with several environmental issues,[1] due to the excessive use of cement and non-renewable natural resources such as aggregates (sand, gravel and pozzolan).[2,3] The production of these cements includes the release of carbon dioxide (CO_2) which leads to global warming.[4,5] It has been shown that for every 1 ton of cement used in construction, more than 900 kg of carbon dioxide (CO_2) is released into the environment,[6]

DOI: https://doi.org/10.37256/sce.5220245166

and also that the energy needed to produce cement comes from non-renewable resources that produce a lot of CO_2.[7] The building sector is extremely energy-intensive, consuming more than 40% of the world's energy,[2-8] with the concerns of environmental impact and climate change.[2] Building requires the use of different types of building materials such as concrete, fired earth bricks, compressed earth bricks, cement bricks, geopolymers bricks, pavements, etc. The fired clay bricks presented good pozzolanic activity[9,10] and alkaline activation.[10,11]

Today, some researchers agree that by 2,060, sand and gravel consumption will have almost doubled worldwide.[12] It is therefore crucial to find alternative solutions for building in a sustainable, economical and environmentally friendly way.[7-15] Similarly, other researchers have shown that most demolition waste from construction and other industrial wastes can be used to replace cement, sand and gravel[16] and therefore require natural aggregates[3] to produce lightweight concrete.[17] These include fired clay bricks debris, eggshells and coconut shells, whose properties are similar to those of cement.[18,19] Durability, low cost, and better strength are very important characteristics of fired bricks.[20] The waste from fired bricks are recycled, preserving new clay deposits and protecting them from the rapid deterioration of the environment.. However, the need for a solution on how to manage these burnt waste bricks is a call of concern. The eggshell and coconut shells (agro waste) are valorized to ensure environmental sustainability by minimizing environmental pollution.

Eggshell, an agro bio-waste material obtained from farmers and found in abundance worldwide is dumped in landfills without any pretreatment thus causing environmental pollution.[21] It contains calcium oxides (carbonate). However, it is applied in domains, such as cement replacement,[22-23] materials for biodiesel,[21-24] and adsorbent in the removal of ionic pollutants and fertilizers.[25] According to standard ASTM specification for limestone,[26] it has good radiation protection properties.[27] Eggshells can be incorporated in cement alongside other materials such as silica fume (SF),[22] rice husk ash (RHA),[28] rice straw ash (RSA),[29] glass powder,[30] palm oil fuel ash (POFA),[31-32] bagasse ash[33] and to contributed to the formation of C-S-H gel.[34-35]

The coconut shell was used as aggregate in the mix composition. Thus, the coconut tree is a very abundant, and renewable resource of energy. The shells are then burnt into ashes in a furnace at a very high temperature to produce the coconut shell ash. It has uniform quality and good resistance to water and fungal attacks. Coconut shell powder is a sustainable building material[36-37] and an eco-friendly alternative to synthetic materials.[38] Coconut shells can be used as materials for making coconut charcoal briquettes, fully biodegradable, low cost, activated charcoal. Coconut shells which is an inexpensive, fully biodegradable activated carbon can be used to make coconut charcoal briquettes. Coconut shells can be replaced or incorporated into cement, such as coconut shell ash (CSA),[39] soil stabilizer,[40] bagasse ash,[41] fine aggregate,[42-43] coarse aggregate,[44-46] and lightweight concrete.[41-47]

This approach to waste management is fully in line with the concept of sustainable development, linked to the circular economy. It could also reduce energy consumption in buildings by 17% and CO_2 emissions by 30%[2] and comply with European Union Directive 2008/98/EC, which sets a recycling target for construction waste of at least 70% by 2020.[48] The circular economy approach therefore remains an innovative solution for providing a sufficiently sustainable raw material with the guarantee of a healthy, waste-free environment.[8]

This study seeks to valorize waste fired bricks used to synthesize ecological compressed earth bricks by using calcined eggshells and coconut shells. It also investigates the mechanical properties such as compressive strength test (σ), water absorption (WA), bulk density (BD), apparent porosity (AP), moisture content (MC) and elastic modulus (EM). Analysis such as Energy Dispersive X-ray analysis (EDX) is used to determine elemental composition and chemical characterization of raw materials and formulated samples. Scanning Electron Microscopy (SEM) is used to determine the morphology of samples, and X-Ray diffraction (XRD) and Fourier Transformed Infrared spectrometry (FT-IR) analysis were carried out to determine the different crystallographic amorphous phases and chemical bonds formed or transformed.

2. Materials and methods

2.1 *Collection and processing of raw materials*

2.1.1 *Grog*

The fired clay bricks debris (CH) (Figure 1 (a)) was obtained from the central region of Cameroon, Mfoundi

Division, more precisely in the locality of Nkolbisson at the artisanal fired clay bricks production unit of the Local Materials Promotion Authority (MIPROMALO). Then they were crushed in a ball mill sieved through a 2 mm sieve and packaged in sealed bags for further analysis. The physical characteristics of grog in this study were carried out on bulk density, effective density, moisture content, porosity, compactness, voids index and fines modulus, respectively. Figure 1 shows the point of collection of raw materials. Figure 1 (a) shows the dumping of grog into the environment; Figure 1 (b) and Figure 1 (c) show eggshells and coconut shells waste. Figure 1 (d) and Figure 1 (f) show the crushing and grinding of coconut shell into coconut shell powder while Figure 1 (e) shows the pretreatment by washing the eggshell and removing all unwanted debris.

2.1.2 *Egg shells*

The egg shells (Figure 1 (b)) were collected from a bakery in the city of Yaounde, Mfoundi Division, in the locality of Etoug-Ebe, Cameroon. Firstly, they were washed in normal water for 15 min to remove any impurities and any unwanted debris from the membrane. It was then sun-dried for 5 days at room temperature (23 ± 3 °C). The egg shells were then oven-dried at 105 ± 5 °C for 2 hrs to remove moisture content from the samples. Raw materials were crushed and sieved at 300 µm to eliminate coarse particles and obtain fine particles. It was later sieved at 75 µm and packaged in hermetically sealed bags. Finally, the white powder obtained was calcined in an electric oven at 900 °C for 2 hrs and noted CO. Its specific gravity used was 2.07-2.50, and the fines modulus is about 1.80.

2.1.3 *Coconut shells*

Coconut shells were collected from coconut sellers on the Yaounde-Douala trunk road at Carrefour Boumnyebel, located in the centre region, Nyong et Kelle Division and Ngog Mapubi district. They were firstly stripped off their fibers, and then crushed using a hammer. Then, they were oven-dried for 24 hrs at 105 ± 5 °C, then crushed and sieved through a 250 µm sieve and finally packaged in a bag and noted CN for further analysis. The specific gravity is 1.33 and the water absorption used is 23%.

Normal tap water was used in all formulations. Precisely the water came from the Cameroon Water Utilities Corporation (Camwater). Its quality complies with the requirements of the Cameroonian standard on compressed earth blocks NC 102-115: 2007.[49] The water is used to bind the matrix components together in paste form and promotes a quick hydration reaction. It must also be pure and free of impurities. The physical properties of raw materials are shown in Table 1.

Table 1. Physical properties of raw materials

Properties	Fired clay bricks debris (CH)	Coconut shells (CN)	Calcined eggshells (CO)	References
Bulk density (g/cm^3)	1.10	0.83	2.07-2.50	Ngayakamo et al.[8]
Effective density (g/cm^3)	2.60	-	-	
Moisture content (%)	1.55	10.57	-	
Water absorption (%)	-	23	-	Lavanya et al.[50]
Porosity (%)	57.66	-	-	
Compactness (%)	42.34	-	-	
Voids index (%)	1.36	-	-	
Finess Modulus	3.67	-	1.80	Muthusamy et al.[51]

Figure 1. Raw materials (a) Collection of grog (b) eggshell (c) coconut shell (d) crushed coconut shell (e) washing of eggshell (f) grinding of raw materials

2.1.4 *Production of mortar samples*

Figure 2 shows formulated samples and preserved samples for further analysis. The earth mortar of dimensions 20 × 20 × 20 mm in size was produced and was obtained from the mixing procedure of water to earth ratio of 2:10. A mass of 360 g was used to make the samples per formulation, as shown in Table 2. The sum of 3 samples was used per formulation and the averages were taken for the calculation of standard deviation.

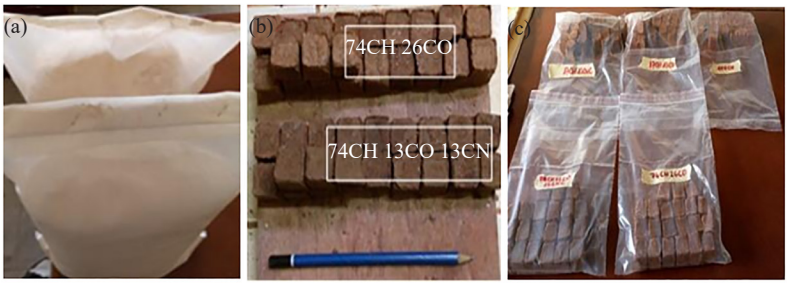

Figure 2. Samples (a) packaged dry samples (b) formulated samples (c) preservation of samples

Table 2. Different mortar formulations

N°	CH (g)	CO 900 °C (g)	CN 250 µm (g)	Label	Code
1	360	0	0	100CH	A
2	313	47	0	87CH 13CO	B
3	313	0	47	87CH 13CN	C
4	266	94	0	74CH 26CO	D
5	266	47	47	74CH 13CO 13CN	E
6	266	0	94	74CH 26CN	F
7	216	144	0	60CH 40CO	G
8	216	97	47	60CH 27CO 13CN	H
9	216	47	97	60CH 13CO 27CN	I
10	216	0	144	60CH 40CN	J
11	313	23.5	23.5	87CH 6.5CO 6.5CN	K
12	241	94	25	67CH 26CO 7CN	L
13	241	25	94	67CH 7CO 26CN	M

2.2 *Methods*

2.2.1 *Energy dispersive X-ray analysis (EDX)*

This analysis enables the various chemical elements present in each inorganic material to be determined quantitatively to determine their chemical composition. An accelerating voltage of 7.5-10 kV was applied during the EDX analysis so that the depth of interaction volume of the electron beam found in the sample is limited. In order to increase the conductivity of the sample (also known as a non-conductive sample) it leads to charging artifacts. A silver-gold coating was applied and images were taken using a backscattered electron detector. 10 images were taken at different positions of each sample and the results obtained were analyzed as averages.

2.2.2 *X-ray diffraction analysis (XRD)*

The XRD is used to qualitatively identify the various crystalline compounds that are present in a material, as well as their crystallographic forms. Ex-situ XRD data was collected on an STOE Stadi-p X-ray powder diffractometer (STOE & Cie GmbH, Darmstadt, Germany) with Cu Kα1 radiation (λ = 1.54056 Å; Gemonochromator; flat samples) in transmission geometry with a DECTRIS® MYTHEN 1K detector (DECTRIS, Baden-Daettwil, Switzerland).

2.2.3 *Fourier transform infrared spectroscopy (FT-IR)*

It is a technique used to assess the nature of molecules in a material as well as impurities. It is based on the absorption phenomenon that occurs when the infrared radiation passes through the matter. This is then selectively observed to depend on the exciting vibrations of the samples, and given that each molecule or group of molecules making up the material has vibration levels corresponding to precise energies. The measurements of infrared spectroscopy are carried out in transmittance and can be an absorbance mode by a spectrometer.

In order to measure the FTIR. A Bruker Vertex 80v having KBr was applied by using 1g of each sample mixed with 200 mg of KBr and pressed at 100 kN using a hydraulic press (ENERPAC P392, USA) to get each pellet. At the range of 400-4,000 cm^{-1} Infrared spectrum of each pellet was recorded at a resolution of 2 cm^{-1} with 32 scans. Samples were recorded using OPUS Spectroscopy software.

2.2.4 *Scanning electron microscopy (SEM)*

The surface of samples was investigated with equipment ZEISS AVO 40 (Carl Zeiss AG, Oberkochen, Germany). After 28 days of curing, the SEM of five samples of mortar coded D (74CH 26CO), E (74CH 13CO 13CN), I (60CH 13CO 27CN), G (60CH 40CO) and F (74CH 26CN) were presented together with XRD and IR data. The samples were examined under an FE-SEM (Nova Nano FE-SEM FEI 450) equipped with an energy dispersive X-ray spectrometer (EDX) and a mapping facility that ran at 15.0 kV in order to evaluate the microstructure. Before examination, tiny fragments of less than 10 mm in size were removed from the center of the samples and dried for 24 hrs in an oven with a temperature control of 50 °C. Following gold coating, fractured surfaces of electrically non-conductive specimens were employed for analysis.

2.2.5 *Mechanical properties of earth mortars*

The various tests carried out on the earth mortars were carried out after 28 days of curing at ambient temperature (23 ± 3 °C). These mechanical properties include bulk density, moisture content, water absorption, apparent porosity, compressive strength and elastic modulus.

2.2.5.1 *Bulk density*

The test consists of weighing each test piece of each sample and calculating the bulk density. In this study, 3 samples of 20 × 20 × 20 mm earth mortar for each formulation were used to determine the average density in accordance with ASTM C642-13.[52] This value is calculated using the formula.

$$BD = \frac{m_1}{v} \quad (1)$$

With BD-bulk density in g/cm^3; m_1-initial mass of sample after 28 days of curing in g; v-volume of sample in cm^3.

2.2.5.2 *Moisture content*

It is carried out on samples from 28 days of curing after 24 hrs in an oven at 105 ± 5 °C. It was used to assess the amount of water evaporated from an average of three samples and can be summarized as shown in equation 2 below:

$$MC = \frac{m_1 - m_2}{m_2} \times 100 \quad (2)$$

Where by m_1= initial mass of sample after 28 days of curing in g;
m_2 = dry mass after 24 hrs in an oven in g.

2.2.5.3 *Water absorption*

It is used to determine the quantity of water retained by a material once it has been soaked in water for 24 hrs in accordance with ASTM standard C642-13,[52] and also gives an idea of the stability of the material in water. The latter is evaluated by the following formula and was determined on an average of three samples:

$$WA = \frac{m_3 - m_2}{m_2} \times 100 \quad (3)$$

Where by m_2 = dry mass after 24 hrs in an oven in g;
m_3 = wet mass after 24 hrs in water in g.

2.2.5.4 *Apparent porosity*

It reveals the porous nature of the material used and provides information on all the voids inside the material. It was determined on an average of three samples using the following formula.

$$AP = \frac{m_3 - m_2}{\rho_e \times v} \times 100 \quad (4)$$

ρ_e-density of water (1 g/cm^3); v-volume of sample in cm^3; m_2-dry mass after 24 hrs in an oven in g; m_3-wet mass after 24 hrs in water in g.

2.2.5.5 *Compressive strength and elastic modulus*

The compressive strength corresponds to the maximum load per unit area above which a material, subjected to this stress under specific conditions and at ambient temperature, can resist before breaking. It was assessed on mortar samples after 28 days of curing and the average was calculated on six samples. While the Elastic modulus provides information on the elasticity and degree of deformation of a material. As with compression strength, the latter was determined at 28 days on an average of 3 samples. It is linked to compressive strength by Hooke's law, which is expressed by the following formula:

$$\sigma = \varepsilon EM \quad (5)$$

with σ-compressive strength in MPa; EM-elastic modulus in MPa; ε-stretching or displacement.

In this research, the mechanical characteristics (compressive strength and elastic modulus) were obtained from tests carried out on a manual extensometer, each time taking a video during the test. Each video was then transformed into images using the Total Video Converter software, and finally, the various points were recorded to plot the curve.

3. Results and discussion

3.1 *X-ray diffraction of raw materials and mortar samples*

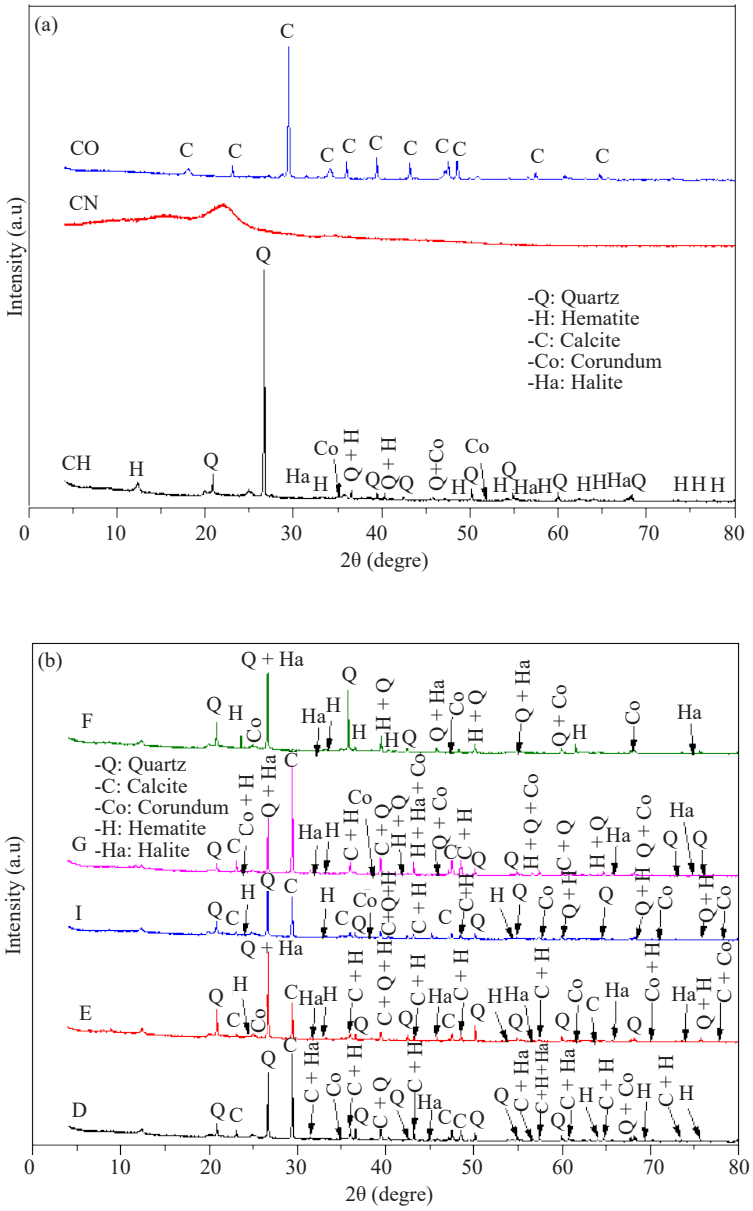

Figure 3. XRD pattern of (a) raw materials (b) mortar samples

Figure 3 shows the X-ray diffraction peaks of grog, coconut shells, and calcined eggshells powder at 900 °C, and mortar samples.

In Figure 3 (a) the characteristic of the grog peak is Quartz (SiO_2) with minor peaks consisting of Halite (NaCl),

Hematite (Fe_2O_3) and Corundum (Al_2O_3). The coconut shell shows no peak while the calcined eggshell powder consists mainly of Calcite ($CaCO_3$) which shows that decomposition by calcination has not been complete and that organic matter is still present in the final product. It observes one more phase as Calcite. As for Figure 3 (b) the samples D, E, I, G and F are all identical, as predicted by EDX analysis. There was no formation of intermediates in any of the five samples as shown below in the XRD spectra:

3.2 *Fourier transform infrared spectroscopy (FT-IR) of raw materials and mortar samples*

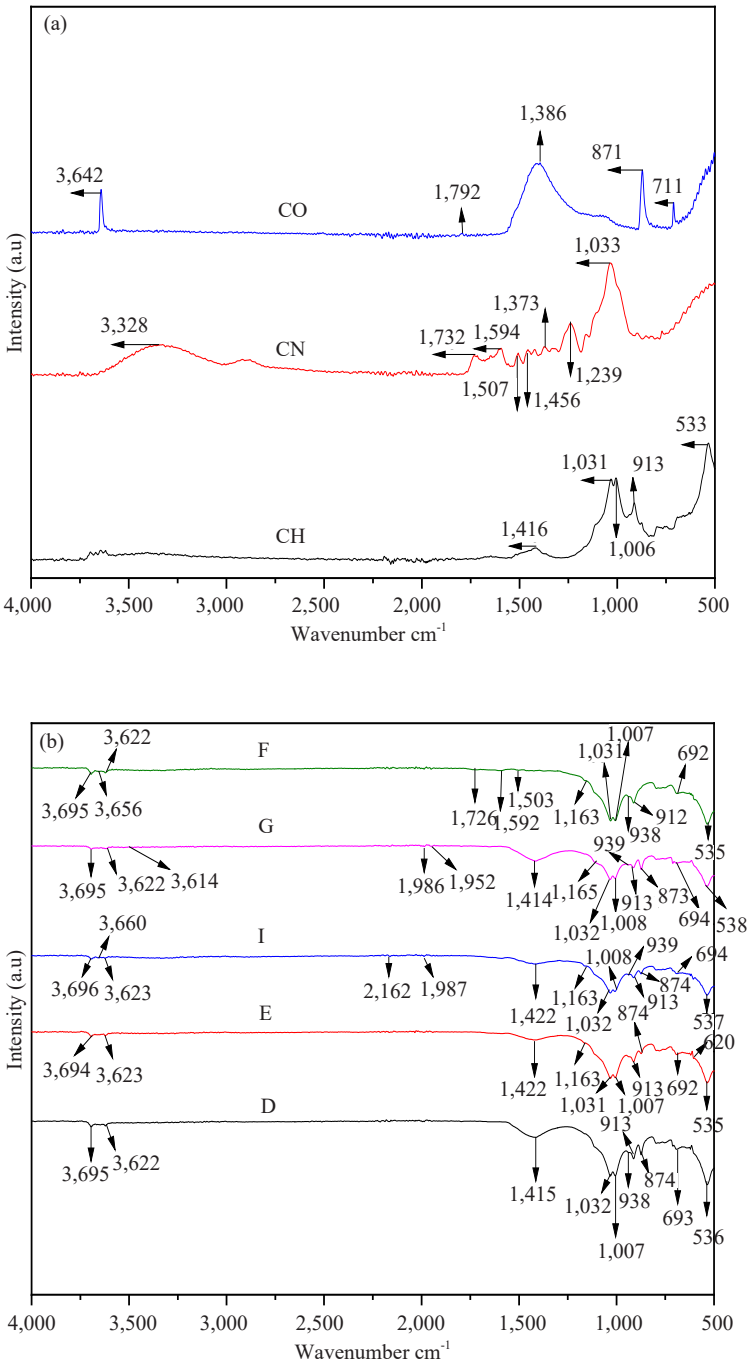

Figure 4. Infrared spectrum (a) raw materials (b) mortar samples

Figure 4 show the IR spectra of the raw materials (grog, coconut shell powder and calcined eggshell powder) and mortar samples (D, E, I, G and F) mentioned above.

According to the work of Amadou,[53] the CH (Figure 4 (a)) infrared spectrum shows a broad, centered main band in the 1,416 cm^{-1} wavenumber region and other bands at 533 cm^{-1} which indicates the vibration of the Si-O-Al group in the material. The region between 1,416 and 1,031 cm^{-1}, the hydroxyl group O-H identified is attributed to the presence of the water molecule due to the humidity of the initial material. In the 1,006 and 913 cm^{-1} regions, the functional groups present are attributed to the Si-O bond in the disordered tetrahedron structure. The band in the region between 913 and 533 cm^{-1} is attributed to the Si-O-Si bond, indicating the presence of quartz in the material.

The IR spectrum of CO (Figure 4 (a)) showed peaks at 3,642 cm^{-1}, 1,792 cm^{-1}, 1,386 cm^{-1}, 871 cm^{-1} and 711 cm^{-1}, revealing the presence of organic matter.[54] More precisely, the peaks at 1,386 cm^{-1}, 871 cm^{-1} and 711 cm^{-1} correspond to the characteristic peaks of calcite obtained after calcination of eggshells at 900 °C.[54] The peak at 1,792 cm^{-1} indicates the presence of C = O carbonyl bonds resulting from calcination while the peak at 3,642 cm^{-1} corresponds to the water (H-O-H) absorbed by the eggshell particles.[54]

As for the IR spectrum of CN (Figure 4 (a)), there is a very broad peak at 3,328 cm^{-1} which indicates the presence of O-H hydroxyl bonds, the peaks at 1,732 cm^{-1}, 1,594 cm^{-1} and 1,239 cm^{-1} are characteristic of C = C bonds, while the peak at 1,033 cm^{-1} corresponds to Si-O bonds which confirms the presence of silica in the material[55] as mentioned in the previous X-ray spectrum. The peak at 1,373 cm^{-1} is attributed to the C-H bonds.[56] The IR spectra of samples D, E, I, G and F (Figure 4 (b)) are all identical in terms of the results obtained. XRD and FTIR results show no compositional chemical differences between the mortar samples,[57] and confirm the formation of identical phases of samples after curing time.[58] These results show the possibility of chemical properties of the crystallinity due to the addition of raw materials.[59] Indeed, XRD and FTIR results revealed that after curing time, crystalline phases initially present in the raw materials were also found in the chemical properties of mortar products justifying their partial formation into the process mixture.[60]

3.3 *Microstructural characterization of raw materials*

EDX and SEM results show the enhancement of the compressive strength, due to the reinforcement of the matrice of mortar synthesized.[61,62] Figure 5 shows the SEM micrograph and EDX spectrum of raw materials such as grog, and coconut shell, as well as eggshell powder calcined at 900 °C. The EDX is a technique that is used for chemical analysis and is associated with the electron microscope based on certain generations of X-ray characteristics that reveal the presence of elements found in the samples.

Figure 5 (a and b) show the EDX and SEM images of grog and presents the chemical components of a higher quantity of Oxygen (51.9%), Silicon (22.8%) and Aluminium (20.7%), moderate quantity of Iron (4.3%) and minor fraction of Sodium (0.4%), respectively. The SEM morphology was carried out at 10, 10, and 10 µm, respectively for grog, calcined eggshell powder and coconut shell, respectively. This was carried out to show the morphology of the agglomerated powder and the irregular shape of the unreacted raw materials found in the matrice. The microstructure showed the major irregular quartz (SiO_2) particles and the unreacted and undissolved particles which are visible around the agglomeration.

Figure 5 (c and d) show the EDX and SEM images of calcined eggshells powder at 900 °C and presents the chemical components as follows: a higher amount of Calcium (61.5%), Oxygen (33.6%) and adequate amount of Carbon (4.9%), respectively. The SEM structure reveals that the eggshell matrices are sponglike in nature. It shows visible pores and calcite irregular shaped particles with porous structure. The microstructure shows a non-uniform size distribution and an irregular shape and indicates the presence of $CaCO_3$. The matrice shows low viscosity which can be explained by the fact that there is low reactivity in the matrice of the raw materials thus causing other raw materials to react slowly since only water was used to activate the formulations.

Figure 5 (e and f) show the EDX and SEM images of coconut shell powder and presents the chemical components of higher quantity of Oxygen (59.7%) and Carbon (36.9%), and moderate quantity of Potassium (3.5%), respectively. The microstructure showed an angular, and fibrous structure. It shows the discrete cell pores and porous nature texture.

Figure 6 shows the SEM images and EDX spectra of the mortar samples that were formulated. Observations show that all these samples are virtually identical and most of them contain Carbon, Oxygen, Sodium, Silicon, Aluminium, Iron and Calcium in varying percentages as shown below in Table 3. Another chemical element, titanium present in only

one sample, had no particular influence on the phase change of the materials after transformation, as confirmed by the XRD spectra of the five previous samples. Figure 6 (b, d, f and j) show that the particles are more or less agglomerated, unlike the particles in Figure 6 (h), which are fractured.

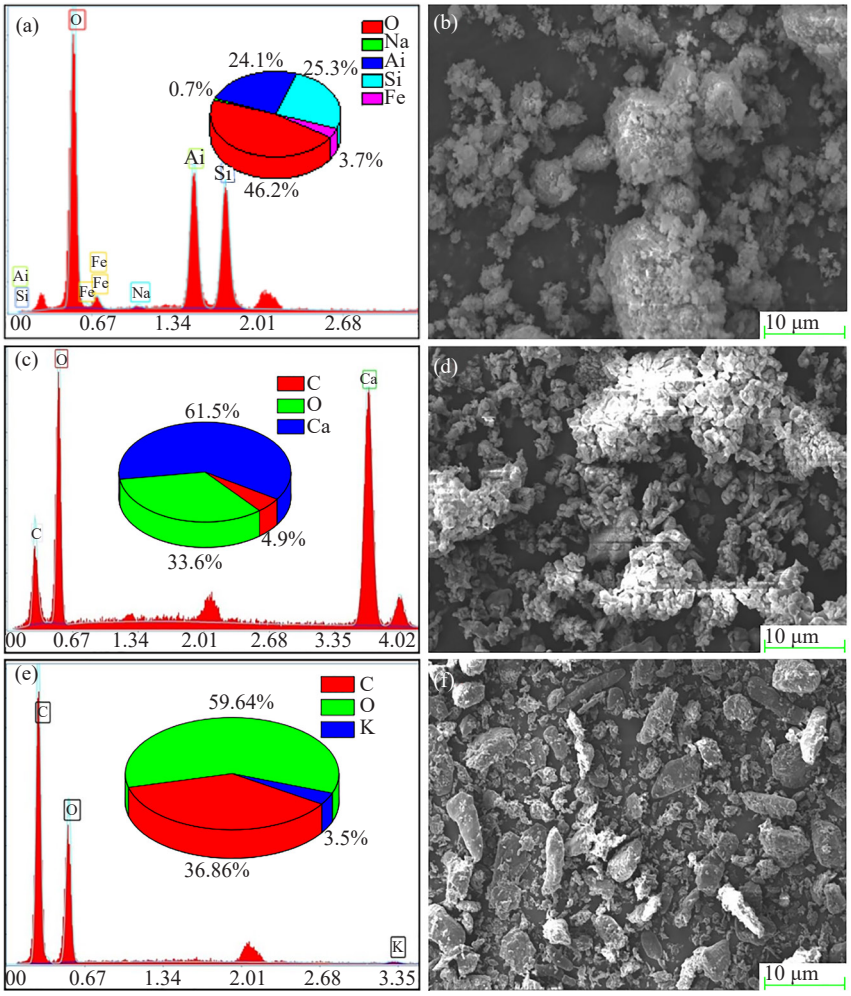

Figure 5. (a, b) EDX spectrum and SEM micrograph of grog (c, d) EDX spectrum and SEM micrograph of calcined eggshells powder (e, f) EDX spectrum and SEM micrograph of coconut shell powder

Figure 6 (a and b) show the EDX and SEM images of D (74CH 26CO) and present the chemical components as follows: higher quantity of Oxygen (47.6%), Silicon (22.8%), Aluminium (11.4%) and Calcium (10.7%), moderate quantity of Iron (6.2%) and minor fractions of Titanium (1%) and Sodium (0.3%), respectively. The SEM structure shows a more compact and homogeneous microstructure.

Figure 6 (c and d) show the EDX and SEM images of E (74CH 13CO 13CN) and presents the chemical components of higher amount of Iron (41.1%), Oxygen (29.9%) and Carbon (10.8%), adequate amount of Aluminium (8.6%) and Silicon (7.3%) and minor fractions of Calcium (1.9%) and Sodium (0.5%), respectively. The SEM structure was carried out to show a dense microstructure and small pores.

Figure 6 (e and f) show the EDX and SEM images of I (60CH 13CO 27CN) and presents the chemical components as follows: higher quantity of Oxygen (43.4%), Carbon (29.5%) and Silicon (12%), moderate quantity of Aluminium (7.8%) and Iron (5.1%) and minor fractions of Calcium (2%) and Sodium (0.3%), respectively. The SEM structure showed a fibrous microstructure.

Figure 6 (g and h) show the EDX and SEM images of G (60CH 40CO) and presents the chemical components

of higher amount of Oxygen (50.3%) and Silicon (46%), minor fractions of Aluminium (1.8%), Calcium (1.5%) and Sodium (0.5%), respectively. The SEM structure was carried out to show a fractured microstructure and minor agglomeration.

Figure 6 (i and j) show the EDX and SEM images of F (74CH 26CN) and presents the chemical components as follows: higher quantity of Oxygen (47.5%), Silicon (26.2%) and Carbon (17.6%), moderate quantity of Aluminium (5.5%) and minor fractions of Iron (3%) and Sodium (0.2%), respectively. The SEM structure showed a porous and an agglomerated microstructure. EDX analysis of formulated samples is shown below in Table 3.

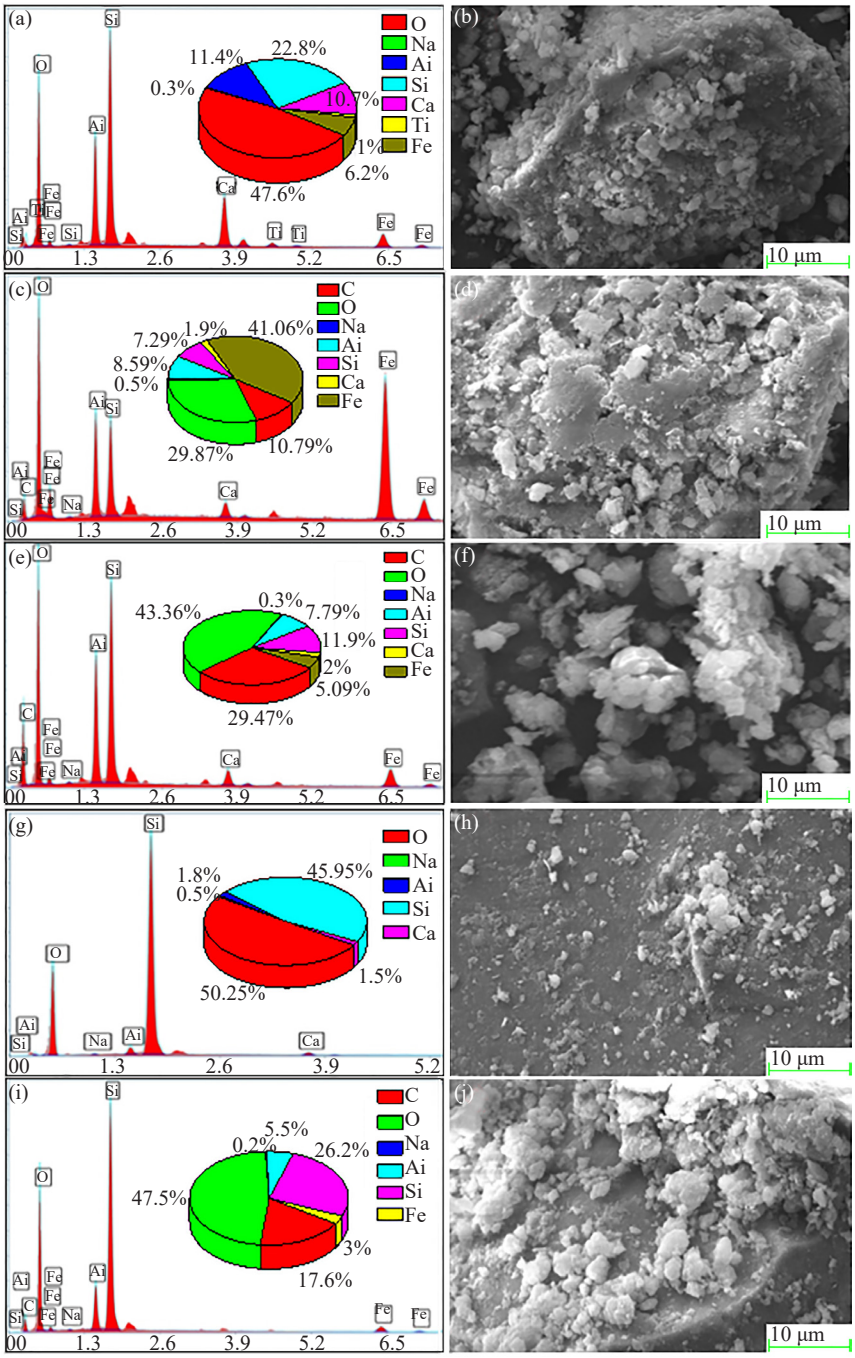

Figure 6. EDX spectrum and SEM micrograph of D (a, b), E (c, d), I (e, f), G (g, h) and F (i, j), respectively

Table 3. EDX analysis of some mortars (formulated samples)

Samples	Chemical components (%)								
	C	O	Na	Si	Al	Fe	Ca	Ti	Total
D	-	47.6	0.3	22.8	11.4	6.2	10.7	1	100
E	10.8	29.8	0.5	7.3	8.6	41.1	1.9	-	100
I	29.5	43.3	0.3	12	7.8	5.1	2	-	100
G	-	50.2	0.5	46	1.8	-	1.5	-	100
F	17.6	47.5	0.2	26.2	5.5	3	-	-	100

While the EDX analysis of various raw materials are represented on Table 4 as shown below.

Table 4. EDX analysis of raw materials

Raw materials	Chemical components (%)								
	C	O	Na	Si	Al	Fe	Ca	K	Total
Grog	-	46.2	0.3	25.3	24.1	3.7	-	-	100
Calcined eggshell	4.9	33.6	-	-	-	-	61.5	-	100
Coconut shell	36.86	59.64	-	-	-	-	-	3.5	100

3.4 *Mechanical properties of earth mortars*

Table 5. Physical and mechanical properties of mortar samples

Formulations	Moisture content (%)	Water absorption (%)	Apparent porosity (%)	Bulk density (g/cm^3)	Compressive strength (MPa)	Elastic modulus (MPa)
A	19.354	0	0	2.3125	1.545	10.897
B	18.75	29.166	58.333	2.375	1.384	8.416
C	21.068	44.220	87.500	2.395	1.522	9.468
D	15.365	29.218	58.333	2.3125	2.701	9.743
E	17.589	40.681	77.083	2.229	1.307	9.749
F	20.229	49.386	91.666	2.229	2.010	8.466
G	13.844	26.579	52.083	2.229	3.885	5.854
H	16.344	34.802	66.666	2.229	0.730	4.955
I	15.708	49.386	91.666	2.145	1.342	9.054
J	18.939	55.559	104.116	2.229	1.342	5.725
K	15.412	40.681	77.083	2.1875	1.166	7.117
L	15.098	34.397	66.666	2.229	0.745	4.394
M	20.191	47.279	87.500	2.229	0.296	3.254

The physical and mechanical properties of samples are represented in Table 5 below while the mechanical properties of earth mortars, in particular, bulk density, moisture content, water absorption, apparent porosity, compressive strength and elastic modulus were determined in this study and presented in Figure 7. Recent studies have reported increased strength in geopolymers containing a large volume of fly ash when cured under high temperatures. Contrarily, few studies show the effects of drying and humidity during the curing process on compressive strength.[63] The properties will be improved by choosing the right mix design for specific applications.[64]

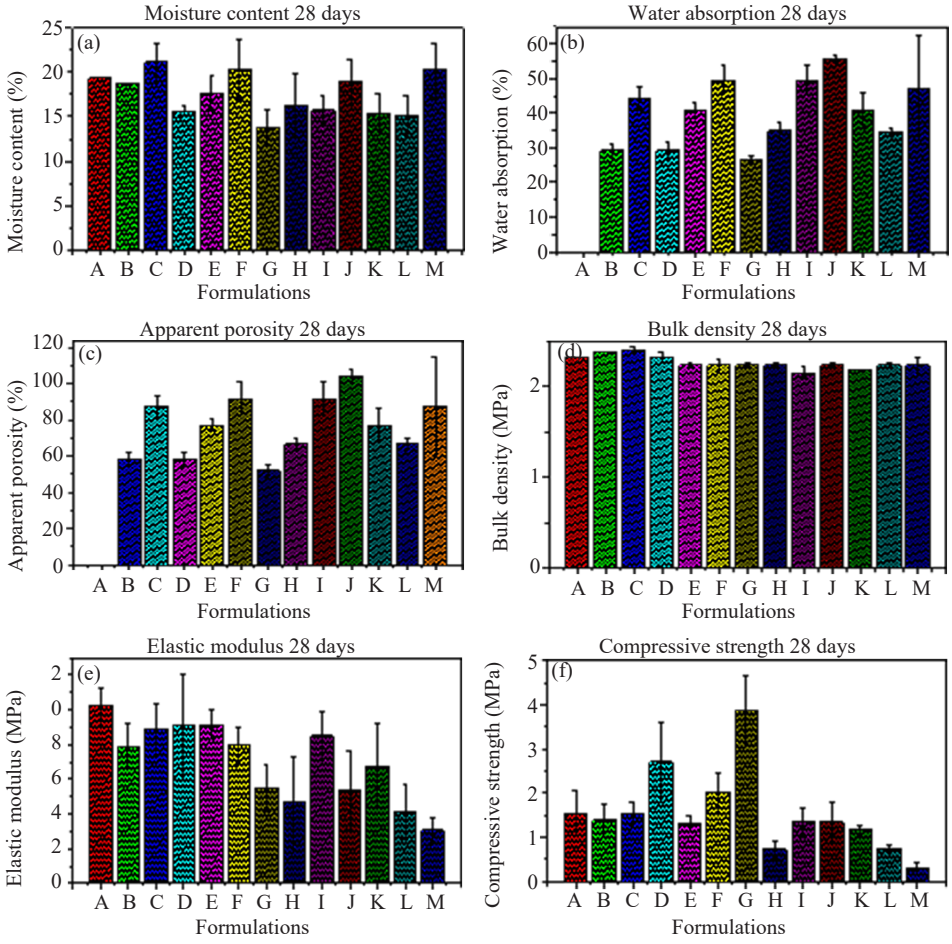

Figure 7. Average curves of mechanical properties (a) moisture content, (b) water absorption, (c) apparent porosity, (d) bulk density, (e) elastic modulus, (f) compressive strength

Figure 7 (a) shows moisture content. For 87CH 13CO, 74CH 26CO and 60CH 40CO, their moisture content includes 18.75, 15.365 and 13.844%, respectively. While for 87CH 13CN, 74CH 26CN and 60CH 40CN are 21.068, 20.229 and 18.939%, respectively. And finally for 74CH 13CO 13CN, 60CH 27CO 13CN, 60CH 13CO 27CN, 87CH 6.5CO 6.5CN, 67CH 26CO 7CN, 67CH 7CO 26CN and 100CH, their moisture content includes 17.589, 16.344, 15.708, 15.412, 15.098, 20.191 and 19.354%, respectively.

Figure 7 (b) shows that with the increase in the percentage of calcined eggshell at 900 °C, and a decrease in the percentages of grog, the water absorption test slightly increases and decreases. For 87CH 13CO, 74CH 26CO and 60CH 40CO the water absorption test increases from 29.166 to 29.218%, and decreases from 29.218 to 26.579%, respectively. While on the other hand, there is an increase in water absorption with an increase in the percentage of coconut shells than an increase from above mentioned formulations for 87CH 13CN, 74CH 26CN and 60CH 40CN with values as 44.220, 49.386 and 55.559%, respectively.

As concerns the mix design of both calcined eggshell and coconut shell the different formulations are given below with their corresponding water absorption for 74CH 13CO 13CN, 60CH 27CO 13CN, 60CH 13CO 27CN, 87CH 6.5CO 6.5CN, 67CH 26CO 7CN, 67CH 7CO 26CN and 100CH there water absorption includes 40.681, 34.802, 49.386, 40.681, 34.397 and 47.279%, respectively. They are greater than 20% and also do not comply with the Draft Cameroonian Standard (less than 20%) for products likely to be exposed to adverse weather conditions, which is justified by the porous nature of the base materials used.

Figure 7 (c) shows apparent porosity. So for 87CH 13CO, 74CH 26CO and 60CH 40CO, their apparent porosity includes 58.333, 58.333 and 52.083%, respectively. While for 87CH 13CN, 74CH 26CN and 60CH 40CN are 87.500, 91.666 and 104.116%, respectively. And finally, for 74CH 13CO 13CN, 60CH 27CO 13CN, 60CH 13CO 27CN, 87CH 6.5CO 6.5CN, 67CH 26CO 7CN and 67CH 7CO 26CN, their apparent porosity includes 77.083, 66.666, 91.666, 77.083, 66.666 and 87.500%, respectively.

Figure 7 (d) shows bulk density. So for 87CH 13CO, 74CH 26CO and 60CH 40CO, their density includes 2.375, 2.3125 and 2.229 g/cm^3, respectively. While for 87CH 13CN, 74CH 26CN and 60CH 40CN are 2.395, 2.229 and 2.229 g/cm^3, respectively. And finally for 74CH 13CO 13CN, 60CH 27CO 13CN, 60CH 13CO 27CN, 87CH 6.5CO 6.5CN, 67CH 26CO 7CN, 67CH 7CO 26CN and 100CH, their bulk density are 2.229, 2.229, 2.145, 2.1875, 2.229, 2.229 and 2.3125 g/cm^3, respectively. However, these values are greater than 1 g/cm^3 and comply with EN 771-1: 2011 standard for protected constructions.[65]

Figure 7 (e) shows elastic modulus. So for 87CH 13CO, 74CH 26CO and 60CH 40CO, their elastic modulus includes 8.416, 9.743 and 5.854 MPa, respectively. While for 87CH 13CN, 74CH 26CN and 60CH 40CN are 9.468, 8.466 and 5.725 MPa, respectively. And finally for 74CH 13CO 13CN, 60CH 27CO 13CN, 60CH 13CO 27CN, 87CH 6.5CO 6.5CN, 67CH 26CO 7CN, 67CH 7CO 26CN and 100CH, their elastic modulus are 9.749, 4.955, 9.054, 7.117, 4.394, 3.254 and 10.897 MPa, respectively.

Figure 7 (f) shows an increase in the percentage of calcined eggshell at 900 °C, with a decrease in the percentages of grog, as the compressive strength increases. For 87CH 13CO, 74CH 26CO and 60CH 40CO the compressive strength test increases to 1.384, 2.701 and 3.885 MPa, respectively. While on the other hand, there is an increase in compressive strength with an increase in the percentage of coconut shells than a decrease from above mentioned formulations for 87CH 13CN, 74CH 26CN and 60CH 40CN with values as 1.522, 2.010 and 1.342 MPa, respectively.

As concerns the mix design of both calcined eggshell and coconut shell, the different formulations are given below with their corresponding compressive strength for 74CH 13CO 13CN, 60CH 27CO 13CN, 60CH 13CO 27CN, 87CH 6.5CO 6.5CN, 67CH 26CO 7CN, 67CH 7CO 26CN and 100CH there strength include: 1.307, 0.730, 1.342, 1.166, 0.745, 0.296 and 1.545 MPa, respectively. The strength starts to increase than later reduces until the last value. The three values of 2.701, 2.010 and 3.885 MPa are higher than the Cameroonian[49] standards (which sets compressive strength at 2 MPa). Thus two of three values 2.701 MPa and 3.885 MPa are higher than the Netherland NEN 3835 standard[66] (which sets compressive strength and falls within the range limit of 2.5-5 MPa). These improved compressive strengths can contribute to the creation of environmental friendly building materials, and promote a circular economy as stated by Nayem,[67] Shivakumar,[68] and also achieve sustainable development of building materials.[69] On the other hand, these results are applied to building and construction materials and decoration as stipulated by Sun et al.[70]

Figure 8 shows the different correlations between mechanical properties (water absorption, apparent porosity, bulk density, moisture content, compressive strength, and elastic modulus) in this study. On the other hand, the correlation coefficients and range limits between properties are shown in Table 6 below.

Table 6. Correlation coefficients and range limits between properties

	Apparent porosity (AP)			Water absorption (WA)			Moisture content (MC)			Elastic modulus (EM)			Bulk density (BD)		
	Code	R^2	Range	Code	R^2	Range	Code	R^2	Range	Code	R^2	Range	Code	R^2	Range
Compressive strength (σ)	a AP	0.58484	0.4-0.6	b WA	0.61373	0.6-0.8	c MC	0.69854	0.6-0.8	d EM	0.66557	0.6-0.8	e BD	0.84998	0.8-1
Water absorption (WA)	a AP	0.99477	0.8-1	-	-	-	b MC	0.81464	0.8-1	c EM	0.85724	0.8-1	-	-	-
Moisture content (MC)	a AP	0.77631	0.6-0.8	-	-	-	-	-	-	b EM	0.95589	0.8-1	-	-	-
Elastic modulus (EM)	AP	0.8246	0.8-1	-	-	-	-	-	-	-	-	-	-	-	-
Bulk density (BD)	a AP	0.62937	0.6-0.8	b WA	0.61717	0.6-0.8	c MC	0.73358	0.6-0.8	d EM	0.67182	0.6-0.8	-	-	-

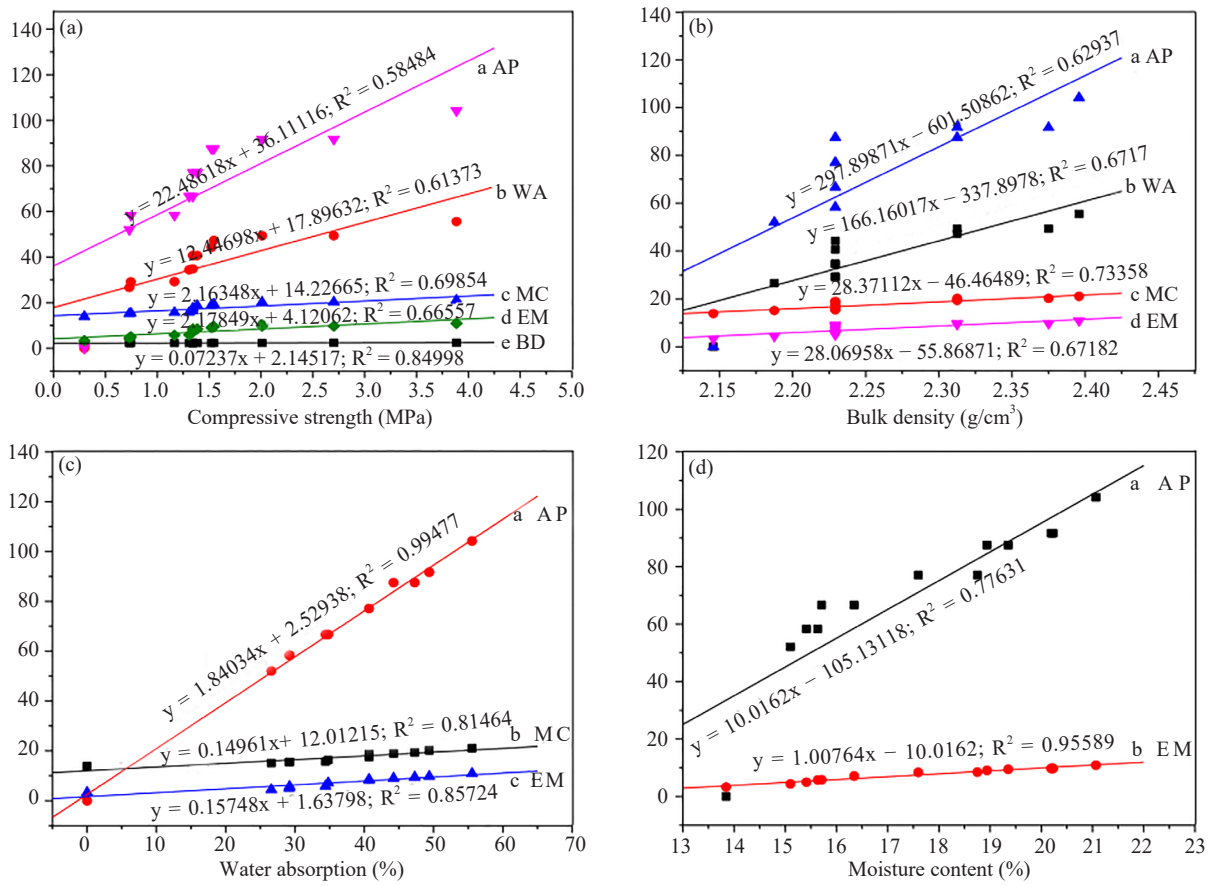

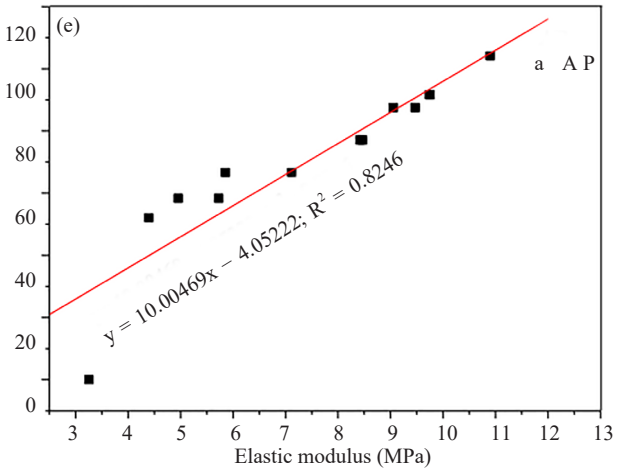

Figure 8. Linear Correlation curves of mechanical properties (a) compressive strength, (b) bulk density, (c) water absorption, (d) moisture content, (e) elastic modulus

Figure 8 shows the linear correlation curves of variation between different mechanical properties such as compressive strength (σ), bulk density (BD), water absorption (WA), moisture content (MC) and elastic modulus (EM). The porosity of different samples was determined by Eq. (4). Figure 8 (a) shows a linear increase in AP, WA, MC, EM, BD with an increase in compressive strength. The correlation coefficients of AP, WA, MC, EM and BD are as follows: 0.58484 (AP), 0.61373 (WA), 0.69854 (MC), 0.66557 (EM) and 0.84998 (BD) respectively. 0.58484 (AP) shows strong correlation and falls between 0.4-0.6. While 0.61373 (WA), 0.69854 (MC) and 0.66557 (EM) show very strong correlation and falls within the range limit of 0.6-0.8 and finally 0.84998 (BD) shows a perfect correlation and falls between the range limit of 0.8-1.

The water absorption of different samples was determined by Eq. (3). Figure 8 (b) shows a linear increase in AP, WA, MC, EM with an increase in bulk density. The correlation coefficients of AP, WA, MC and EM are as follows: 0.62937 (AP), 0.6717 (WA), 0.73358 (MC) and 0.67182 (EM) respectively. 0.62937 (AP), 0.6717 (WA), 0.73358 (MC) and 0.67182 (EM) show very strong correlation and fall within the range limit of 0.6-0.8.

The moisture content of different samples in this study was calculated by Eq. (2). Figure 8 (c) shows a linear increase in AP, MC, EM with an increase in water absorption. The correlation coefficient of AP, MC and EM are as follows: 0.99477 (AP), 0.81464 (MC) and 0.85724 (EM) respectively. 0.99477 (AP), 0.81464 (MC) and 0.85724 (EM) show perfect correlation and falls within the range limit of 0.8-1.

The density of different samples was determined by Eq. (1). Figure 8 (d) shows a linear increase in AP, EM with an increase in moisture content. The correlation coefficients of AP and EM are as follows: 0.77631 (AP) and 0.95589 (EM) respectively. 0.77631 (AP) shows very strong correlation and falls between the range limit of 0.6-0.8. While 0.95589 (EM) shows perfect correlation and falls within the range limit of 0.8-1.

The elastic modulus of different samples in this work was determined by Eq. (5). Figure 8 (e) shows a linear increase in AP with an increase in elastic modulus. The correlation coefficient of AP is as follows 0.8246 (AP), its shows perfect correlation and falls between 0.8-1.

Linear correlation curves were engaged by other researchers. Ardakani et al.[71] who worked on "The relation between particle density and static elastic moduli of lightweight expensed clay aggregates" and established a linear correlation between elastic modulus and bulk density, and their results showed a correlation coefficient of 0.96 indicating a perfect correlation. On the other hand, Shen et al.[72] determined more linear correlations between compressive strength and apparent porosity with different moisture contents. They also obtained a correlation coefficient of 0.90 for all relationships which is a perfect correlation. However, Cobîrzan et al.[73] showed a correlation coefficient between compressive strength and bulk density of 0.89564 and it's a perfect correlation which is also in agreement with the above study.

4. Conclusion

The aim of this work was to valorize fired clay brick waste (grog) used to produce ecological compressed earth bricks by using calcined eggshells and coconut shells for sustainable building. The results showed that the compressive strength increases with an increase in the percentage of calcined eggshells at 1.38, 2.70, and 3.88 MPa, respectively. Moisture content decreases with an increase in the percentage of calcined eggshell and coconut shell. Water absorption and elastic modulus slightly increase and decrease with an increase in the percentage of calcined eggshell. Apparent porosity and bulk density were decreased with the percentage of calcined eggshell increase. The microstructure analysis shows an agglomerated structure and a dense microstructure due to the presence of calcium silicate hydrate (C-S-H) gel formation that leads to high compressive strength. The chemical composition shows that all samples are identical. This work shows that the addition of different percentages of calcined eggshell and coconut shell has greatly improved the physico-mechanical and engineering properties of samples.

Conflict of interest

The authors declare there is no conflict of interest at any point with reference to research findings.

References

[1] Rahul, C. R.; Prasad, C. V. S. R.; Poloju, K. K.; Al Muharbi, N. M. J.; Arun, Y. V. An experimental investigation on mechanical properties of concrete by partial replacement of cement with wood ash and fine sea shell powder. *Materials Today: Proceedings* **2020,** *13*, 1325-1330.

[2] Kouta, N. *Mechanical behavior and characterization : Durability of new materials based on clay*; Bordeaux, 2020.

[3] Rasool, D. A.; Abdulkarem, M. A.; Jasem, M. H. Improvement of the cement mortar properties using recycled waste materials. *Inter. Jour. Nano. Mat.* **2022,** *15*, 155-162.

[4] Prakash, R.; Thenmozhi, R.; Raman, S. N.; Subramanian, C.; Divyah, N. Mechanical characterisation of sustainable fibre-reinforced lightweight concrete incorporating waste coconut shell as coarse aggregate and sisal fibre. *Inter. Jour. Env. Sci. Tech.* **2021,** *18*, 1579-1590.

[5] Amin, M. N.; Ahmad, W.; Khan, K.; Al-Hashem, M. N.; Deifalla, A. F.; Ahmad, A. Testing and modeling methods to experiment the flexural performance of cement mortar modified with eggshell powder. *Case Stud. Const. Mat.* **2023,** *18*, 1-16.

[6] Duchesne, J. Alternative supplementary cementitious materials for sustainable concrete structures: A review on characterization and properties. *Waste Biomass Valor* **2021,** *12*, 1219-1236.

[7] Eid, J. *Development of an Eco-Geo-Material Based on Raw Earth*; University of Havre, 2016.

[8] Ngayakamo, B.; Onwualu, A. P. Recent advances in green processing technologies for valorisation of eggshell waste for sustainable construction materials. *Heliyon* **2022,** *8*, 41-49.

[9] Pitarch, A. M.; Reig, L.; Tomás, A. E.; Forcada, G.; Soriano, L.; Borrachero, M. V.; Paya, J.; Monzo, J. M. Pozzolanic activity of tiles, bricks and ceramic sanitary-ware in eco-friendly portland blended cements. *Jour. Clean Prod.* **2021,** *279*, 123713.

[10] García-Díaz, A.; Delgado-Plana, P.; Bueno-Rodríguez, S.; Eliche-Quesada, D. Investigation of waste clay brick (chamotte) addition and activator modulus in the properties of alkaline activation cements based on construction and demolition waste. *Jour. Buil. Eng.* **2024,** *84*, 1-23.

[11] Ge, X.; Hu, X.; Li, H.; Shi, C. Synergistic effect of characteristics of raw materials on controlling the mechanical properties of fly ash-based geopolymers. *Cem. Concr. Compo.* **2024,** *145*, 105368.

[12] Oberle, B.; Bringezu, S.; Hatfield-Dodds, S.; Hellweg, S.; Schandl, H.; Clement, J. *Global Resources Outlook 2019: Natural Resources for the Future We Want*; Nairobi: A Report of the International Resource Panel, 2019.

[13] Atta, I.; Bakhoum, E. S. Environmental feasibility of recycling construction and demolition waste. *Int. J. Environ Sci. Te.* **2024,** *21*, 2675-2694.

[14] Kamwa, T. A. R.; Tome, S.; Chongouang, J.; Eguekeng, I.; Spieß, A.; Fetzer, A. N. M.; Kamseu, E.; Janiak, C.; Etoh, M. A. Stabilization of compressed earth blocks (CEB) by pozzolana based phosphate geopolymer binder: Physico-mechanical and microstructural investigations. *Cleaner Materials* **2022,** *4*, 1-10.

[15] Sinkhonde, D. Analytical solutions of surface porosity of waste brick powder specimens from different milling conditions: A path towards sustainability. *Next Sustainability* **2023,** *2*, 1-13.
[16] Priya, S. S.; Padmanaban, I. Effect of coconut shell ash as an additive on the properties of green concrete. *Global NEST Jour.* **2023,** *25*, 1-9.
[17] Prakash, R.; Divyah, N.; Srividhya, S.; Avudaiappan, S.; Amran, M.; Raman, S. N.; Guindos, P.; Vatin, N. I.; Fediuk, R. Effect of steel fiber on the strength and flexural characteristics of coconut shell concrete partially blended with fly ash. *Materials* **2022,** *15*, 1-22.
[18] Bhartiya, A.; Dubey, M. Replacement of cement with coconut shell ssh and egg shell powder for preparation of fresh concrete. *Inter. Res. Jour. Eng. Tech.* **2018,** *5*, 1272-1275.
[19] Chong, B. W.; Rokiah, O.; Ramadhansyah, P. J.; Doh, S. I.; Li, X. Properties of concrete with eggshell powder: A review. *Phys. Chem. Earth* **2020,** *120*, 102951.
[20] Rathinavel, N.; Kannadasan, K.; Ismail, A. A. M.; Mammo, W. D.; Alagar, M. Impact of eggshell powder on the mechanical and thermal properties of lightweight geopolymer. *Adv. Civ. Eng.* **2023,** *6*, 1-11.
[21] Alsharari, F.; Khan, K.; Amin, M. N.; Ahmad, W.; Khan, U.; Mutnbak, M.; Houda, M.; Yosri, A. M. Sustainable use of waste eggshells in cementitious materials: An experimental and modeling-based study. *Case Stud. Const. Mat.* **2022,** *17*, 1-15.
[22] Rizalman, A. N.; Sibin, B. Characterization and strength activity index of eggshell powder and silica fume as partial cement replacement. *Key Eng. Mat.* **2023,** *943*, 225-231.
[23] Shi, X. C.; Shui, Z. Effect of eggshell powder addition on the properties of cement pastes with early CO_2 curing and further water curing. *Jour. Const. Buil. Mat.* **2023,** *404*, 133231.
[24] Goli, J.; Sahu, O. Development of heterogeneous alkali catalyst from waste chicken eggshell for biodiesel production. *Ren. Ener.* **2018,** *128*, 142-154.
[25] Faridi, H.; Arabhosseini, A. Application of eggshell wastes as valuable and utilizable products: A review. *Res. Agri. Eng.* **2018,** *64*, 104-114.
[26] ASTM, A. Standard Specification for Quick Lime, Hydrated Lime, and Limestone for Selected Chemical and Industrial Uses. In *ASTM Standard*; West Conshohocken, PA, 2011; pp 6-8.
[27] Souadi, G.; Bulcar, K.; Yucel, A.; Oglakci, M.; Sezer, S.; Madkhali, O.; Depci, T.; Topaksu, M.; Can, N. Radiation-induced thermoluminescence in $Ca_5(PO_4)_3OH$ powder from eggshell: Trapping parameter assessment. *Radia. Phys. Chem.* **2024,** *217*, 111488.
[28] Adetoro, A. E.; Oladapo, A. S.; Oluborode, K. D. Impact of rice husk ash on compressed cement-lateritic brick durability and microstructural characteristics. *World Jour. Adv. Res. Rev.* **2022,** *14*, 617-622.
[29] Hakeem, I. Y.; Amin, M.; Agwa, I. S.; Abd-Elrahman, M. H.; Ibrahim, O. M. O; Samy, M. Ultra-high-performance concrete properties containing rice straw ash and nano eggshell powder. *Case Stud Const Mat.* **2023,** *19*, e02291.
[30] Chen, Z.; Amin, M. N.; Iftikhar, B.; Ahmad, W.; Althoey, F.; Alsharari, F. Predictive modelling for the acid resistance of cement-based composites modified with eggshell and glass waste for sustainable and resilient building materials. *Jour. Buil. Eng.* **2023,** *76*, 107325.
[31] Alnahhal, A. M.; Alengaram, U. J.; Yusoff, S.; Singh, R.; Radman, M. K. H.; Deboucha, W. Synthesis of sustainable lightweight foamed concrete using palm oil fuel ash as a cement replacement material. *Jour. Buil. Eng.* **2021,** *35*, 102047.
[32] Mujedu, K. A.; Ab-Kadir, M. A.; Ismail, M. A review on self-compacting concrete incorporating palm oil fuel ash as a cement replacement. *Const Buil Mat.* **2020,** *258*, 119541.
[33] Mishra, M.; Mekro, R.; Jamir, L.; Ete, M.; Oniya, T.; Kalita, A. Experimental investigation for stabilization of expansive soil by using waste materials eggshell powder and bagasse ash. In *Proceedings of SECON'23.* SECON 2023. *Lecture Notes in Civil Engineering, vol 381*; Nehdi, M.; Hung, M. K.; Venkataramana, K.; Antony, J.; Kavitha, P. E.; Beena, B. R., Eds.; Springer, Cham., 2024; pp 345-353.
[34] Azhar, M. O. *Combined Effect of Eggshell and Ceramic Waste Powder as Partial Cement Replacement in Wheat Straw Reinforced Concrete*; Capital University of Science and Technology, 2023.
[35] Pinheiro, V. D.; Alexandre, J.; Xavier, G. C.; Marvila, M. T.; Monteiro, S. N.; de Azevedo, A. R. G. Methods for evaluating pozzolanic reactivity in calcined clays: A review. *Materials* **2023,** *16*, 1-28.
[36] Manikanta, A.; Kumar, P. K.; Udaya, T.; Lakshmi, I. P. R.; Kumar, K. R. Evaluation of concrete with glass and coconut shell in place of coarse aggregate and partially replaced cement. *Inter Jour Innov Res Comp Sci Tech.* **2022,** *5*, 145-148.
[37] Kumarasamy, K.; Gunasekaran, K.; Ramasamy, A. Elucidation of microstructural and mechanical properties of coconut husk mortar as a sustainable building material for ferrocement. *Sustainability* **2023,** *15*, 1-32.

[38] Krumar, K. V.; Daniel, C.; Amudhan, V.; Kapilan, S.; Arunraj, E. Experimental investigation of eco-friendly building blocks utilizing coconut shells. *Mater. Today Proc.* **2023**.
[39] Reddy, B. D.; Babu, M. M.; Jyothy, S. A.; Kumar, N. K.; Reddy, P. N.; Kavyateja, B.V.; Kumar, K. H. Strength and durability of concrete by partial replacement of cement by fly ash and fine aggregates by granite dust. *Mater. Today Proc.* **2023**.
[40] Kamaruddin, F.; Jaya, A. A. M.; Md Roslee, M. H.; Ahmad, A.; Abdullah, M. S. A study on crushed coconut shells as stabilizer to soil. *IOP Conference Series: Earth Env Sci.* **2023,** *1238*, 1-10.
[41] Srivani, G.; Mohan, U. V. Study on strength properties of concrete by partial replacement of cement with sugarcane bagasse ash and coarse aggregate with coconut shell. *Mater. Today Proc.* **2023**.
[42] Azunna, S. U.; Aziz, F. N. A. A.; Cun, P. M.; Elhibir, M. M. O. Characterization of lightweight cement concrete with partial replacement of coconut shell fine aggregate. *SN Appli Sci.* **2019,** *649*, 1-9.
[43] Raja, K. C. P.; Thaniarasu, I.; Elkotb, M. A.; Ansari, K.; Saleel, C. A. Shrinkage study and strength aspects of concrete with foundry sand and coconut shell as a partial replacement for coarse and fine aggregate. *Materials* **2021,** *14*, 1-19.
[44] Natarajan, K. S.; Ramalingasekar, D.; Palanisamy, S.; Ashokan, M. Effect on mechanical properties of lightweight sustainable concrete with the use of waste coconut shell as replacement for coarse aggregate. *Env. Sci. Pollut. Res.* **2022,** *29*, 39421-39426.
[45] Stel'makh, S. A.; Beskopylny, A. N.; Shcherban, E. M.; Mailyan, L. R.; Meskhi, B.; Shilov, A. A.; El'shaeva, D.; Chernil'nik, A.; Kurilova, S. Alteration of structure and characteristics of concrete with coconut shell as a substitution of a part of coarse aggregate. *Materials* **2023,** *16*, 1-19.
[46] Sujatha, A.; Balakrishnan, S. D. Properties of high strength lightweight concrete incorporating crushed coconut shells as coarse aggregate. *Mater. Today Proc.* **2023**.
[47] Hasan, N. M. S.; Habibur, M.; Sobuz, R.; Shaurdho, N. M. N.; Basit, M. A.; Paul, S. C.; Meraz, M. M.; Saha, A.; Miah, M. J. Investigation of lightweight and green concrete characteristics using coconut shell aggregate as a replacement for conventional aggregates. *Inter. Jour. Civ. Eng.* **2023,** *22*, 37-53.
[48] Thang, L.; Sébastien, R.; Saout, L.; Eric, G. Fresh behavior of mortar based on recycled sand-Influence of moisture condition. *Const Buil Mat.* **2016,** *106*, 35-42.
[49] *NC 102-115 Cameroonian Standards for Compressed Earth Blocks*; 2007.
[50] Lavanya, B. A.; Sunitha, M. S.; Umesha, P.; Chethan, H. H. Experimental study of partial replacement of cement and coarse aggregate with fly ash and coconut shell. *Inter. Res. Jour. Eng. Tech.* **2018,** *5*, 194-198.
[51] Muthusamy, K.; Kamaruzaman, A. M.; Ruslan, H. N.; Ismail, M. A. Properties of sustainable concrete consisting crushed eggshell waste as fine aggregate replacement. *Construction* **2023,** *3*, 207-214.
[52] ASTM, A. *Standard Test Method for Density, Absorption, and Voids in Hardened Concrete*; ASTM International, 2013.
[53] Amadou, P. *Elaboration and Characterization of Aluminosilicate Refractory Bricks Based on Clay Materials from Koutaba and Mayouom (Western Region): Effect of Adding Coffee Production Residues and Rice Husks*; Yaoundé, 2020.
[54] Ngayakamo, B. H.; Bello, A.; Onwualu, A. P. Development of eco-friendly fired clay bricks incorporated with granite and eggshell wastes. *Env Chal.* **2020,** *1*, 1-28.
[55] Lazim, Z. M.; Hadibarata, T. Adsorption characteristics of bisphenol a onto low-cost modified phyto-waste material in aqueous solution. *Water Air Soil. Pollut.* **2015,** *226*, 1-11.
[56] Bello, O. S.; Adegoke, K. A.; Fagbenro, S. O.; Lameed, O. S. Functionalized coconut husks for rhodamine B dye sequestration. *Appli Water Sci.* **2019,** *9*, 1-15.
[57] Montoya-Escobar, N.; Ospina-Acero, D.; Velásquez-Cock, J. A.; Gómez-Hoyos, C.; Serpa, G. A.; Gañan, R. P. F.; Vélez, A. L. M.; Escobar, J. P.; Correa-Hincapié, N.; Triana-Chávez, O.; et al. Use of fourier series in X-ray diffraction (XRD) analysis and fourier-transform infrared spectroscopy (FTIR) for estimation of crystallinity in cellulose from different sources. *Polymers* **2022,** *14*, 1-16.
[58] Bajaj, S.; Keche, P. A.; Patade, R. S.; Khedkar, V. M.; Shinde, S. Structural properties of $CoFe_{2-x}Ce_XO_4$ (x = 0.00 and 0.02) nanoparticles using XRD and FTIR analysis. *Int. J. Adv. Manuf. Technol.* **2020,** *3*, 524-531.
[59] Poralan Jr, G. M.; Gambe, J. E.; Alcantara, E. M.; Vequizo, R. M. X-ray diffraction and infrared spectroscopy analyses on the crystallinity of engineered biological hydroxyapatite for medical application. *IOP Conf. Series: Mat. Sci. Eng.* **2015,** *79*, 1-6.
[60] Nouping, F. J. N.; Kaze, C. R.; Linda, L. D.; Ghazouni, A.; Ndassa, M. I.; Kamseu, E.; Rossignol, S.; Leonelli, C. Effects of curing cycles on developing strength and microstructure of goethite-rich aluminosilicate (corroded

laterite) based geopolymer composites. *Mater. Chem. Phys.* **2021,** *270*, 1-17.
[61] Garg, R.; Bansal, M.; Aggarwal, Y. Strength, rapid chloride penetration and microstructure study of cement mortar incorparating micro and nano silica. *Int. J. Electrochem. Sci.* **2016,** *11*, 3697-3713.
[62] Althoey, F.; Awoyera, O. P.; Inyama, K.; Khan, A. M.; Mursaleen, M.; Hadidi, M. H.; Najm, M. H. Strength and microscale properties of bamboo fiber-reinforced concrete modified with natural rubber latex. *Mater. Chem. Front.* **2022,** *9*, 1-14.
[63] Ikeo, Y. Effect of Curing Conditions on strength development of geopolymer mortar using fly ash and ground granulated blast furnace slag. *Takenaka Technical Research Report* **2019,** *75*, 1-7.
[64] Verma, N. K.; Rao, M. C.; Kumar, S. Effect of curing regime on compressive strength of geopolymer concrete. *IOP Conf. Series: Environ. Earth Sci.* **2022,** *982*, 1-13.
[65] *NF EN 771-1 Standard Specification for Masonry Units: Clay Bricks*; 2011.
[66] *NEN 3835 Mortars for masonrywork of bricks, blocks or elements of fired clay, calcium silicate, concrete and aerated concrete*; 1991.
[67] Nayem, N. H. The potential of sustainable materials for green building practices. *Am. J. Civ. Eng.* **2023,** *3*, 30-35.
[68] Shivakumar, G. S. Green building materials. *IJSREM Journal* **2023,** *12*, 1-8.
[69] Hu, Y.; Wang, J.; Wang, X. Application of green building materials in the field of construction and sustainable development. *E3S Web of Conferences* **2021,** *308*, 1-7.
[70] Sun, P.; Zhang, X. Application of green building materials in civil engineering construction. *AIP Conference Proceedings* **2019,** *2073*, 1-4.
[71] Ardakani, A.; Yazdani, M. The relation between particle density and static elastic moduli of lightweight expanded clay aggregates. *Appli Clay Sci.* **2014,** *93*, 28-34.
[72] Shen, J.; Xu, Q. Effect of moisture content and porosity on compressive strength of concrete during drying at 105 °C. *Const. Buil. Mat.* **2019,** *195*, 19-27.
[73] Cobîrzan, N.; Thalmaier, G.; Balog, A. A.; Constantinescu, H.; Timis, I.; Streza, M. Thermophysical properties of fired clay bricks with waste ceramics and paper pulp as pore-forming agent. *Jour. Therm. Anal. Calor.* **2018,** *134*, 843-851.